Pergamon

PII: S0191-8141(96)00088-0

Journal of Structural Geology, Vol. 19, No. 2, pp. 225 to 241, 1997

0191-8141/97 $17.00+0.00

The high temperature static recovery and recrystallization behaviour of cold-worked Carrara marble

S. J. COVEY-CRUMP

Rock and Ice Physics Laboratory, Department of Geological Sciences, University College London, Gower Street, London WC1E 6BT, U.K.

(*Received* 13 *March* 1996; *accepted in revised form* 4 *October* 1996)

Abstract—The static recovery and recrystallization behaviour of Carrara marble has been investigated as a function of pre-strain (8–27%) and annealing temperature (500–700°C). Quantitative estimates of the rate of recovery were obtained by comparing the stress/strain curves generated at a temperature of 426°C, a confining pressure of 170 MPa, and a strain-rate of 3×10^{-4} s^{-1} before and after a period of isostatic annealing. Curves of fractional recovery (r) as a function of log time (t) show a characteristic sigmoidal shape in which the rate of recovery ($dr/d \log t$) is initially small, increases rapidly, and finally becomes small again. The acceleration of recovery occurs at shorter times both with increasing pre-strain and with increasing annealing temperature. Microstructural examination of the annealed material shows that the acceleration of recovery corresponds to the onset of recrystallization, and that prior to the onset of recrystallization, recovery is controlled by the development of a subgrain structure, whereas after recrystallization has gone to completion, it is controlled by the intensification and growth of this substructure.

The results have been interpreted within the perspective of Hart's state variable description of inelastic deformation. This analysis shows that the decay of the mechanical state of the marble during annealing can be treated as a two stage static recovery process (substructure formation→substructure coarsening), with the recrystallization marking the transition between these two stages.

INTRODUCTION

It is widely recognized that the mechanical properties and microstructures of previously deformed materials are profoundly modified by subsequent isostatic annealing if the temperatures are sufficiently high for the rates of solid state diffusion processes to be significant over the time scale of interest. In the metallurgical sciences, considerable experimental effort has been directed towards providing a detailed account of the nature and rates of such modifications in order to optimize the thermomechanical treatments given to metals and alloys and thereby their resulting properties (Kwon and DeArdo, 1990; Laasraoui and Jonas, 1991; Martin *et al.*, 1993). However, there has as yet been little attempt to conduct similar work on geological materials despite the clear implications that such work would have (a) for formulating more accurate descriptions of material properties for use in geophysical deformation models than have hitherto been used, and (b) for interpreting natural deformation microstructures which have been affected by post-kinematic annealing.

This paper presents results from an experimental programme designed to investigate the evolution of the mechanical properties and microstructures of previously deformed samples of Carrara marble during isostatic annealing at temperatures between 500 and 700°C. Both the experimental strategy adopted and the analysis of the results obtained have been conducted from the perspective of the state variable description of inelastic deformation due to E. W. Hart (Hart, 1976). This was for the following two reasons.

(1) It is observed in metals that the response to annealing is sensitive to the thermomechanical history of the annealing material (e.g. the strain-rate and temperature of the prior deformation, the loading configuration), and consequently the resulting descriptions of that response tend to be both complex and specific to particular thermomechanical histories. For metals, the problem of history dependence is to some extent mitigated by conducting experiments which are simulations of the intended thermomechanical treatments. However, for geological materials the prohibitive time-scale involved makes this strategy impossible, and hence the problem of finding a history-independent description of the response to annealing assumes a greater importance. Hart's state variable description of inelastic deformation offers a solution to this problem by defining an internal state variable which provides a measure of the mechanical state of a material in terms of the current magnitudes of the deformation variables (e.g. differential stress, strain-rate, temperature), irrespective of the thermomechanical history.

(2) The inelastic (i.e. crystal plastic) deformation properties of materials, and not merely their annealing behaviour, is, in general, dependent upon their prior thermomechanical history. Hart's description of inelastic deformation is just one of several internal state variable descriptions devised in the material sciences to accommodate this history dependence (see Miller, 1987 where five of these descriptions are reviewed and compared). These descriptions differ from each other in the manner in which they balance the mutually competitive requirements of providing the most accurate description of

material properties possible while minimizing the experimental difficulties associated with evaluating the material parameters in the description. For geological materials the experimental problem is particularly acute because in order to suppress cataclasis, the requisite experiments must be conducted at elevated confining pressures, and this in turn imposes severe technical limitations on the quality of data that can be obtained. Indeed, the experimental difficulties are such that for geological materials history dependence is usually ignored, and steady state flow laws are used to describe experimental data. The significance of this steady state approximation for the results of geophysical deformation modelling remains unclear in the absence of any alternative flow laws which can be used in the models to produce a comparative set of results. In an attempt to determine if recent improvements in triaxial deformation apparatus design permit more sophisticated flow laws to be evaluated, Covey-Crump (1992, 1994) attempted to evaluate Hart's description of inelastic deformation for Carrara marble. Hart's description was chosen from among the alternatives merely because it is the simplest to evaluate. In this previous work, experiments were conducted on Carrara marble at a confining pressure of 200 MPa in the temperature range 120–400°C, and it was found that extremely well-constrained values of the parameters in Hart's equations could be obtained. However, Hart's description is only fully formulated for conditions where deformation alone can change the mechanical state of the deforming material. This restricts its applicability to temperatures at which annealing type processes are not rate-significant, i.e. effectively to temperatures less than about half the melting point of the material concerned (although the precise range of applicability depends upon the self-diffusion kinetics of that material). This is a severe restriction because (a) most of the significant natural inelastic deformation occurs at higher temperatures, and (b) most of the important constituents of the lithosphere (e.g. quartz, feldspar, pyroxene, olivine) must be deformed at higher temperatures in the laboratory if cataclasis is to be avoided at experimentally accessible strain-rates. At issue therefore, is whether to attempt to accommodate deformation-independent changes in mechanical state into Hart's description, thereby allowing it to be extended to higher temperatures, or whether to abandon that description in favour of an alternative internal state variable description which is more general but more difficult to evaluate. By examining how the mechanical state variable in Hart's description is affected by the operation of annealing type processes, the aim is to explore the potential of the former option.

Since Hart's description of inelastic deformation forms the perspective in which the experiments reported here have been conducted, in the following account the salient features of that description are briefly outlined before the experimental programme itself is described.

HART'S DESCRIPTION OF INELASTIC DEFORMATION

Hart's description of inelastic deformation has been described in detail elsewhere (Korhonen *et al.*, 1987; Covey-Crump, 1992, 1994), and hence only those aspects of it that are of particular significance to the present study are described here. These concern three matters:

(1) an explanation of what the variable that describes the mechanical state actually is;

(2) an account of the small strain behaviour of the description (which is significant for the problem of evaluating the change in mechanical state induced by a period of annealing); and

(3) an account of the nature of the problem of extending the description to higher temperatures.

Hart's mechanical state variable

In his original analysis, Hart (1970) determined the conditions that must be satisfied if a mechanical equation of state for plastic (i.e. time-dependent, non-recoverable, non-brittle) deformation is to exist. He restricted himself to the stable, homogeneous deformation of an isotropic material under a uniaxially applied stress (all of which restrictions have been subsequently removed), and assumed both that the contribution of grain boundary sliding to the plastic strain was negligible, and that the mechanical condition of the deforming material was influenced only by the deformation. During any isothermal deformation history under these restrictions, the variation of the plastic strain α with the applied differential stress σ and the plastic strain-rate $\dot{\alpha}$ in some increment of time can be written as

$$d\alpha = A\mathrm{d}\ln\sigma + Bd\ln\dot{\alpha}, \tag{1}$$

where A and B are material parameters. Equation (1) merely describes the smooth variation of any of the deformation variables in terms of the others. It follows that a state variable description of plastic deformation exists if equation (1) is an exact differential. Now if A and B are unique functions only of σ and $\dot{\alpha}$, equation (1) is a so-called Pfaffian form in two variables and consequently there always exists an integrating factor, here of the form $\Gamma(\sigma, \dot{\alpha})$, such that

$$\Gamma d\alpha = A\Gamma\mathrm{d}\ln\sigma + B\Gamma d\ln\dot{\alpha}, \tag{2}$$

is an exact differential (Sneddon, 1957). Hence the necessary and sufficient conditions for the existence of a state variable description of plastic deformation are that A and B are unique functions only of σ and $\dot{\alpha}$, i.e. that they do not depend on the deformation history. If this is found to be the case then by defining

$$d\ln\sigma^* = \Gamma d\alpha = A\Gamma\mathrm{d}\ln\sigma + B\Gamma d\ln\dot{\alpha}, \tag{3}$$

a state variable $\sigma^*(\sigma, \dot{\alpha})$ can be introduced which describes the mechanical state of the deforming material.

It also follows from the theory of Pfaffian forms that if one integrating factor Γ exists, then so do an infinity of others. Hence any scheme for assigning σ^* a numerical value is arbitrary.

Subject to the restrictions Hart placed on his analysis, the conditions for the existence of a state variable description of plastic deformation have been shown to be satisfied for every material so far investigated (which includes a wide range of metals, ceramics and simple ionic solids, Korhonen *et al.*, 1987). The analysis places no constraints on the functional form of the mechanical equations of state constituting that description. Rather these were left for empirical determination. The subsequent experimental effort led to two plastic equations of state, applicable in different stress regimes, which Hart combined with a description of anelastic (i.e. time-dependent, recoverable, non-brittle) deformation to form his general model of grain matrix (i.e. no grain boundary sliding) inelastic deformation (Hart, 1976). The position of the boundary between the two stress regimes changes with deformation, and so in formulating the deformation model it proved convenient to identify σ^* as the magnitude of the stress at that boundary.

A less mathematical definition of σ^* follows from a micromechanical interpretation of the deformation model (Hart, 1984). The dislocation flux responsible for grain matrix inelastic deformation can be treated as being influenced both by the passage of dislocations through strong barriers to their motion (such as are presented by dislocation tangles and other discrete defects), and by the kinetics of glide through regions of relatively obstacle-free crystal (which is governed by the intrinsic lattice resistance to dislocation motion). At large stresses, dislocations can surmount the strong barriers to their motion by mechanically activated processes, and so the kinetics of dislocation 'glide' are deformation-rate controlling. At lower stresses (but above the yield stress), dislocations pile up behind the barriers and can only be overcome with the aid of strongly thermally activated processes. Since such thermally activated processes require a wait-time at the barriers, the rate of barrier penetration/circumvention is then deformation-rate controlling. Hart was able to show that the two empirically determined plastic equations of state were of a functional form which could describe respectively these two types of rate-controlling behaviour. By identifying the mechanical state variable as the magnitude of the stress at the boundary between these two deformation-rate controlling regimes, σ^* effectively becomes equivalent to the mechanical threshold stress, i.e. the stress above which a significant number of dislocations in the deforming material can mechanically overcome the strong barriers to their motion. As such it is therefore some measure of the 'size' and spatial distribution of those barriers. So far, however, there have been few attempts to correlate experimentally determined values of σ^* with microstructural observations to determine the nature of this measure, and how it might relate to quantifiable features of the microstructure, e.g. mobile/immobile/total dislocation density, the dislocation cell/subgrain size, although preliminary observations suggest there that is a systematic correspondence with these variables (Alexopoulos *et al.*, 1982; Stone, 1991).

Small strain behaviour

Hart's model provides an excellent description of inelastic deformation beyond the plastic yield point, but predicts yielding behaviour which is much more sharply defined than is found in real materials, i.e. it does not describe the small amount of permanent strain (commonly described as microplastic strain) which accumulates in most materials at stresses above the elastic limit but below that required for macroplastic yielding (Alexopoulos *et al.*, 1981). The difficulty derives from the use of only one variable to describe the mechanical state.

In the model, Hart envisages that at low stresses (but greater than the elastic limit), dislocations pile up behind the strong barriers to their motion but cannot overcome them. A stored strain is produced which is recovered on release of the stress as the dislocations return to their original positions. Since this strain is time-dependent and recoverable it is properly referred to as anelastic. At higher stresses dislocations can overcome the barriers, but when the stress is released they are prevented from returning to their original positions by those same barriers, and are thereby responsible for a permanent plastic strain. Since the model accounts for the post-yield behaviour well, σ^* must be some measure of the 'size' and spatial distribution of the most significant barriers. However, there is no reason why there should not be a size continuum of smaller barriers which may be overcome at stresses greater than the elastic limit but lower than that required for macroplastic yielding, and which would thereby lead to the microplastic strain.

The modifications to Hart's model required to accommodate these so-called weak barriers have been made by introducing a second mechanical state variable as some description of the 'size'/spatial distributions of these weaker barriers (Jackson *et al.*, 1981). These modifications are only significant at very small strains (typically less than 1 or 2%) and it is beyond the capability of currently available triaxial deformation apparatus to evaluate the material parameters in the accompanying extra constitutive equations at such small strains at high confining pressure. However, because from size considerations it is reasonable to suppose that the weak barrier network is more easily affected by annealing-type processes than the strong barrier network, the potential influence of weak barriers on the shape of the initial part of stress/strain curves is a significant consideration when, as is conventionally the case, the change in mechanical properties occurring during a given annealing period is estimated using the shape of the initial part of the stress/strain curve generated on a previously annealed sample (see below).

Extending Hart's model to high temperatures

As indicated above, Hart's deformation model is only fully formulated for conditions where deformation alone can change the mechanical state of the deforming material. However, at high homologous temperatures, annealing-type recovery processes influence the mechanical state of a material. In order to extend the model to higher temperatures it is therefore necessary to find some function that describes this influence.

A recovery process is, by definition, one that provides a negative contribution to the athermal work-hardening rate. The athermal work hardening rate is a measure of the rate of increase of elastic strain energy that accompanies the accumulation of dislocations in the deforming material. Hence any process which either removes dislocations or rearranges them into a lower energy configuration is a recovery process. Recovery processes requiring the presence of a differential stress are conventionally referred to as *dynamic*; those which do not require a differential stress as *static*. In practice the distinction is not always easy to apply: many of the recovery processes occurring during deformation which are conventionally described as dynamic without regard as to whether they actually require a differential stress to be operative may in fact be more conveniently considered in mechanistic terms as static recovery processes which simply operate at faster rates during deformation because the deformation maintains high levels of internal strain energy.

Of interest in the present context are static recovery processes. The driving force for such processes are the local elastic stresses arising from the presence of lattice defects. Such elastic stresses may cause (a) dislocation motion, leading to the annihilation of those dislocations of opposite sign which meet each other, and to the rearrangement of dislocations into a low energy configuration (i.e. into a subgrain network), and (b) boundary migration (i.e. recrystallization), leading to the elimination of dislocations in the migrating boundary.

In formulating his original deformation model, Hart left scope to incorporate the influence of static recovery processes on the mechanical state of a material. He wrote the evolution of mechanical state as

$$\mathrm{d}(\ln \sigma^*)/\mathrm{d}t = \dot{\alpha}\Gamma - \Re, \qquad (4)$$

where $\dot{\alpha}$ is the plastic strain-rate, Γ is the integrating factor of equation (2) which describes the change in σ^* with strain as a function of the deformation variables (i.e. it incorporates both the athermal work hardening and dynamic recovery contributions to the evolution of σ^*), and $\Re$ describes the time rate of change in σ^* due to nominally deformation independent recovery processes. By definition, $\Re$, the static recovery function, is a function only of the thermomechanical history experienced by the recovering material (which in Hart's analysis is encompassed in the magnitude of σ^*), and of temperature.

In the temperature range in which Hart originally formulated his model $\Re = 0$. Hence he made no attempt to specify the functional form of $\Re$. The only previous experimental investigation of $\Re$ was conducted on Type 316 stainless steel but the results were complicated by the formation of precipitates during annealing (Yamada, 1977). Given equation (4), it follows that if Hart's model is to be extended to high temperatures, knowledge of $\Re$ is significant not only in itself, but also for determining the form of Γ at high temperatures.

EXPERIMENTAL METHODS

The most widely employed method of investigating static recovery behaviour is by means of the interrupted constant displacement-rate test. In this test the specimen is first loaded at constant displacement-rate to a given strain. It is then off-loaded and subjected to the desired annealing conditions. After some prescribed annealing period the specimen is then either recovered for microstructural analysis, or is reloaded under the original deformation conditions to determine the amount of recovery that has occurred during the anneal. This simple experimental strategy was adopted for this study.

In order to investigate the static recovery function $\Re$, it is necessary to determine the time-rate of change of σ^* during annealing as a function of both the magnitude of the mechanical state and the annealing temperature. The experimental problem is therefore one of deforming samples to various mechanical states and determining the mechanical state after the annealing period as a function of annealing temperature and duration. Evaluation of the mechanical state requires the use of a material for which Hart's equations of state have been fitted. For these reasons the experimental programme was conducted on Carrara marble for which Hart's equations have been shown to provide an excellent description of the inelastic deformation behaviour up to 400°C (Covey-Crump, 1992, 1994).

Starting material

All the specimens used in the experimental programme were cored from a single block of Carrara marble that was obtained from a monument mason. This was the same block of marble as used in the experiments reported by Covey-Crump (1994) and Rutter (1995). The marble is a white, granoblastic, calcite marble with a mean grain-size (lineal intercept size) of 147 μm. The grain boundaries are well defined but non-planar. There are minor deformation features; most grains show some undulatory extinction, many contain a few deformation twins, and there is a weak shape fabric, but there is no crystallographic preferred orientation. The calcite is 99.76% pure with respect to solute impurities, the principal impurities being Mg 2250 wt ppm and Sr 97 wt ppm (as determined by inductively coupled plasma spectroscopy).

Dark grey inclusion trails, composed of widely disseminated, very fine-grained opaques and fluid inclusions, form a prominent feature of the hand specimen. Where these are particularly concentrated, the calcite grain size may be reduced to as little as 25 μm, but this is only rarely the case. Approximately ten percent of the specimens contained one or two isolated euhedral crystals of quartz, albite or white mica of similar grain-size to the calcite.

The experiments were conducted on right circular cylindrical specimens, 6.35 mm in diameter and approximately 16 mm long, obtained by coring the marble block in an arbitrary but constant direction. This was in the same direction as in the previous studies on material from this block (Covey-Crump, 1994; Rutter, 1995), i.e. with the core axis inclined at approximately 60° to the weak flattening fabric. Care was taken to avoid the dark grey streaks in the marble as far as possible. After coring the specimens were placed in an oven at 80°C until required for use.

General experimental procedure

All the experiments were performed using an externally heated, fluid (water) medium, triaxial deformation apparatus designed and constructed by E. H. Rutter and R. F. Holloway and incorporating an internal load cell (Rutter and Brodie, 1988; Covey-Crump, 1992). To isolate the specimens from the confining medium they were contained within annealed, commercial purity copper sleeves of 0.25 mm wall thickness. The data reduction procedures used to analyze the data generated during the deformation part of the experiments were exactly as described by Covey-Crump (1994). As in that previous work, all strains quoted here are logarithmic strains.

The deformation part of every experiment was conducted in axial compression at a constant displacement-rate of 0.3 mm min^{-1} (corresponding to a strain-rate of approximately 3×10^{-4} s^{-1}). The confining pressure during both the deformation and isostatic annealing parts of the experiments was 170 MPa. In all the experiments the deformation was conducted at 426°C. This is approximately the maximum temperature for which nominally deformation-independent changes in mechanical state are undetectable over the duration of the deformation (Covey-Crump, 1992), and hence is approximately the maximum temperature for which the fitted equations of state can be used to determine the mechanical state of the deformed samples. The choice of the highest possible deformation temperature reflects the need to deform at a temperature as near to the annealing conditions as possible to minimize the duration of the heating period immediately prior to the anneal, and thereby to minimize both the recovery occurring during heating and the duration of the shortest practicable anneal period. In each experiment the anneal duration was specified from the instant the annealing temperature was attained until the instant cooling was commenced. Heating from the deformation temperature was conducted as rapidly as possible (with a consequent annealing temperature overshoot of ≈ 10°C), but took up to 40 min (depending on the annealing temperature), with a further 30 min required for the attainment of thermal equilibrium. Hence 3 h was arbitrarily selected as the minimum anneal duration for which the heating transient effects could be ignored in those experiments designed to quantify the recovery.

About 80 interrupted constant displacement-rate experiments were conducted to quantify the recovery occurring during annealing. In these experiments the amount of recovery occurring as a function of anneal duration was investigated for:

(1) a given anneal temperature (611°C) after different pre-strains (logarithmic strains of 0.08, 0.17 and 0.27); and

(2) a given pre-strain (0.17) at different anneal temperatures (509, 560, 611, 661 and 712°C).

In each suite of experiments six annealing periods were investigated, equally spaced in log-time between 3 h and 40 days. The values of pre-strain and temperature investigated span the maximum range available given the experimental technique. The minimum pre-strain that could be investigated was constrained to be 0.06 by the area method of estimating the amount of recovery during annealing (see below). The maximum pre-strain was constrained to be less than 0.3 because at larger strains the assumption of homogeneous deformation used in the data reduction procedures (Covey-Crump, 1994) begins to become too inaccurate to permit meaningful stresses and strains to be determined. The temperatures are those at the centre of the sample, as measured by a chromel–alumel thermocouple located about 15 mm above the top of the sample and corrected to compensate for the different position of the thermocouple with respect to the furnace hot-spot. The temperature gradient along the sample was less than 2°C. The maximum temperature was constrained by the apparatus design, while the minimum temperature was constrained to be that for which recovery was measurable over the timescale of the experiments.

About a further 90 experiments were conducted to investigate the microstructural evolution during annealing. These microstructural changes were determined as a function of

(1) anneal duration at different annealing temperatures (560, 611, 661 and 712°C) after a given pre-strain (0.17); and

(2) anneal duration at a given annealing temperature (611°C) after different pre-strains (0.08, 0.17 and 0.27).

In these experiments up to thirteen annealing periods were investigated, equally spaced in log-time between a few minutes and 50 days. The microstructural observations were all made on double-polished, ultra-thin sections using a standard optical polarizing light microscope.

Quantifying the recovery

The amount of recovery occurring during an annealing period may be quantified by comparing the stress/strain curve generated from the annealed sample with that generated under the same conditions at the same cumulative strain (i.e. including the deformation prior to the annealing) on a sample which has not been annealed. Three methods of making such comparisons have been widely employed in the metallurgical literature (Fig. 1). The first is a stress based comparison in which the fractional recovery is defined as

$$\sigma_{rec} = (\sigma_3 - \sigma_2)/(\sigma_3 - \sigma_1), \tag{5}$$

where σ_1 is the yield stress in the initial loading, σ_2 the yield stress in the reloading, and σ_3 the flow stress that would have pertained at the cumulative strain at which yielding occurred in the reload had the test not been interrupted for annealing. The second is an area based comparison in which the fractional recovery is defined as

$$A_{rec} = (A_3 - A_2)/(A_3 - A_1), \tag{6}$$

where A_1 is the area under the initial loading curve in a given strain interval, A_2 the area under the reloading curve in the same strain interval, and A_3 the area under the loading curve that would have pertained in the same cumulative strain interval as used to determine A_2 had the test not been interrupted. The third comparison defines the fractional recovery as

$$\epsilon_{rec} = \Delta\epsilon/\epsilon, \tag{7}$$

where ϵ is the final strain attained in the first loading, and $\Delta\epsilon$ is the translation parallel to the strain axis that is required to superpose the reloading stress/strain curve on to the uninterrupted curve.

After static recovery the shape of the initial part of the reloading stress/strain curves is generally found to be influenced by reloading transients which decrease the observed stress at given reload strain. Consequently, because the stress, area, and strain based estimates are evaluated using progressively larger strain parts of the reloading curve, then $\sigma_{rec} > A_{rec} > \epsilon_{rec}$. All three recovery estimates were evaluated in this study. The stresses used in equation (5) were those corresponding to the following strains

σ_1; total strain 0.01

σ_2; reload strain 0.01

σ_3; total strain $= \epsilon - \epsilon^{(e)} + 0.01$

where $\epsilon^{(e)}$ is the elastic component of the strain at the end of the pre-anneal loading as calculated from the stress supported at that strain using the Young's modulus of calcite. The choice of the stress supported at a strain of 0.01 for the 'yield' stresses in equation (5) is arbitrary. The areas used in equation (6) were calculated from the areas under the stress/strain curves between the following strains

A_1; total strain = 0.01 and total strain = 0.06

A_2; reload strain = 0.01 and reload strain = 0.06

A_3; total strain $= \epsilon - \epsilon^{(e)} + 0.01$
and total strain $= \epsilon - \epsilon^{(e)} + 0.06$

The use of a strain interval of 0.05 represents an arbitrary compromise between having as large an interval as possible to minimize reloading transient effects, while recognizing that the size of the interval dictates the minimum pre-strain that can be investigated (i.e. the minimum pre-strain must be larger than the upper strain bound on the interval). $\Delta\epsilon$ used in equation (7) was determined by visual inspection using that part of the reloading curve unaffected by the reloading transients (generally at reload strains of greater than 0.05).

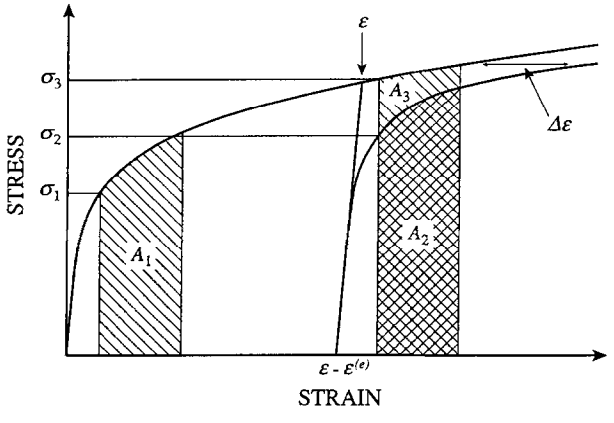

Fig. 1. Definition of the terms in equations (5)–(7) which are used to compare the constant displacement-rate stress/strain curve generated from an unannealed sample with that generated after annealing, and which thereby permit the recovery occurring during the isostatic annealing period of an interrupted constant displacement-rate test to be quantified.

Determining the change in mechanical state

The existence of reloading transients complicates the evaluation of the change in mechanical state σ^* occurring over a given anneal period. As noted above, within the context of the micromechanical rationale of Hart's deformation model, reloading transients may be ascribed to the recovery of the weak barrier network. However, also as noted above, it is the strong barriers that control the magnitude of σ^*. Consequently, it is important that the estimate of σ^* immediately after annealing is determined using portions of the reloading curve for which the transient effects are negligible. Hence of the three conventional recovery estimates the most suitable for calculating $\Delta\sigma^*$ is ϵ_{rec}.

Of the three recovery estimates ϵ_{rec} is the one most

susceptible to the experimental uncertainties, of which the most significant is the performance of the apparatus force gauge. This is because the slope of the Carrara marble stress/strain curve at the deformation conditions is sufficiently small at large strains for small variations in the reproducibility of the stress supported by the various specimens at given strain (typically ± 4 MPa in this study) to have a large effect on the determination of $\Delta\epsilon$, whereas uncertainties of similar magnitude have only a small effect on the computation of σ_{rec} and A_{rec}. The significance of this problem is a strong function of the amount of recovery (being greater when the recovery is small because $\Delta\epsilon$ is then estimated using relatively high strain parts of the stress/strain curve). To minimize this problem, an empirical correlation between the magnitudes of σ_{rec}, A_{rec} and $\epsilon_{\rm rec}$ was determined using every experiment for which these estimates were evaluated. Then for any given experiment the correlation was used with the values of σ_{rec} and A_{rec} for that experiment to calculate the value of ϵ_{rec} for use in determining $\Delta\sigma^*$. In this way all the recovery information was utilized to determine the change in mechanical state.

At the deformation conditions the mechanical equation of state for the inelastic deformation of Carrara marble is

$$\sigma = \sigma^* \exp[-(\dot{\epsilon}^*/\dot{\epsilon}^{\lambda})], \tag{8}$$

where

$$\dot{\epsilon}^* = (\sigma/G)^m f_0 \exp(-H/RT), \tag{9}$$

in which λ, m, f_0 and H are material constants, G is the rigidity modulus, R is the gas constant, σ is the differential stress, $\dot{\epsilon}$ is the inelastic strain-rate, and T is the temperature. Using the following values of the material parameters (Covey-Crump, 1994)

$$\lambda = 0.2;\ m = 9.170;\ f_0 = 2.367 \times 10^{20}\ \mathrm{s}^{-1}$$

$$H = 165.3\ \mathrm{kJmol}^{-1};\ G = 27582\ \mathrm{MPa}$$

and

$$\dot{\epsilon} = 3 \times 10^{-4}\ \mathrm{s}^{-1};\ T = 699\ \mathrm{K}$$

and rewriting equation (8) as

$$0 = \ln\sigma^* - \ln\sigma - [(f_0/\dot{\epsilon})\exp(-H/RT)^{\lambda}[G]^{-\lambda m}[\sigma^*]^{\lambda m}, \tag{10}$$

then σ^* may be determined for any value of σ by using the Newton–Raphson method. Because the experiments were conducted at constant displacement-rate and not constant strain-rate, the actual strain-rate in the initial loadings varied between 3×10^{-4} and $4 \times 10^{-4}\ \mathrm{s}^{-1}$ depending on the initial specimen length and strain, but the error introduced here is small in comparison with the other measurement and fitting errors. The stresses used in equation (10) were all determined from a reference stress/strain curve generated from a specimen loaded at the standard deformation conditions to a strain in excess of 0.3. The magnitude of σ^* immediately before annealing was given by the stress supported at a total strain of ϵ on the reference curve; the magnitude of σ^* immediately after annealing by the stress supported at a total strain of $(\epsilon - \Delta\epsilon)$ on that curve.

RESULTS

Quantitative estimates of recovery

The values of σ_{rec}, A_{rec} and ϵ_{rec} obtained in this investigation are listed in Table 1. The errors on these estimates are difficult to assess. It has been shown using samples from the same block of Carrara marble used in this study but deformed using a different triaxial deformation apparatus, that the stress supported at any given strain for different samples deformed under identical conditions is reproducible to within 1%, i.e. that any variability between the specimens has negligible mechanical significance (Covey-Crump, 1992, 1994). However, there are (a) measurement errors peculiar to the deformation apparatus used in this study, primarily arising from a variation in the reproducibility of the force gauge output between loadings under identical conditions, (b) errors introduced by very minor changes in sample configuration (e.g. axial alignment of the sample) during unloading and reloading, and uncertainties in the strength of the copper jacket around the specimen after annealing, and (c) real modifications in the material behaviour as a result of any microstructural changes occurring during annealing (e.g. in the crystallographic preferred orientation, or in the grain size). The nature of the interrupted constant displacement-rate test is such that these sources of error are only visible indirectly because it is implicit in the test that the annealed material behaves exactly as an unannealed specimen would at the equivalent strain $(\epsilon - \Delta\epsilon)$. However, the fact that beyond the reloading transient the superposition of the reload stress/strain curves on the reference stress/strain curve is good (Fig. 2), suggests that in this study the second and third of these sources of error were of limited mechanical significance. Moreover, the fact that the recovery estimates in Table 1 show a smooth and systematic variation with anneal duration, annealing temperature and pre-strain also suggests that the errors are small.

The recovery estimates in Table 1 are plotted as a function of log anneal duration in Fig. 3, each estimate being plotted for the two cases of constant annealing temperature/various pre-strains and constant pre-strain/various annealing temperatures. The recovery curves given by each estimate show qualitatively the same features: a shallow short time portion, a steep intermediate time portion and a shallow long time portion. The steep portion of these curves is displaced to shorter times with increasing pre-strain and increasing annealing

Table 1. Experiments conducted to determine the evolution of mechanical state during the isostatic annealing of cold-worked Carrara marble

	t (s)	σ_{rec}	A_{rec}	ϵ_{rec}	σ^*(MPa)
		$T=611°C$; $\epsilon=0.08$			
	0	0	0	0	287
†CR53	11520	0.63	0.46	0.06	256
†CR49	61854	0.75	0.51	0.06	252
CR43	229120	0.76	0.59	0.25	240
CR52	231567	0.75	0.59	0.25	240
CR48	503548	0.78	0.60	0.37	240
CR46	925400	0.80	0.61	0.25	239
CR54	1017144	0.85	0.72	0.66	220
CR50	2222487	0.93	0.75	0.62	217
		$T=611°C$; $\epsilon=0.175$			
	0	0	0	0	349
CR23	11423	0.72	0.50	0.29	314
CR21	15388	0.78	0.52	0.26	313
CR45	61548	0.76	0.54	0.40	309
CR18	235963	0.87	0.68	0.46	287
CR24	495420	0.96	0.76	0.63	272
CR17	1109465	1.03	0.86	0.71	245
CR12	2795938	1.02	0.89	0.81	234
		$T=611°C$; $\epsilon=0.2725$			
	0	0	0	0	385
CR40	11040	0.70	0.49	0.50	350
CR44	65918	0.85	0.65	0.62	328
CR41	239956	1.06	0.84	0.71	287
CR47	936747	1.04	0.93	0.88	249
CR55	2987020	1.08	0.95	0.91	241
		$T=509°C$; $\epsilon=0.175$			
	0	0	0	0	349
CR28	13346	0.34	0.21	0.14	337
CR26	60223	0.49	0.31	0.26	331
CR35	63372	0.56	0.35	0.34	329
CR27	244726	0.45	0.30	0.26	331
CR34	946538	0.61	0.40	0.26	324
CR32	952624	0.62	0.37	0.23	328
CR30	2060936	0.58	0.42	0.37	320
		$T=560°C$; $\epsilon=0.165$			
	0	0	0	0	344
CR62	10690	0.48	0.28	0.15	330
CR61	60464	0.57	0.38	0.33	321
CR68	218780	0.59	0.42	0.36	316
CR59	928266	0.62	0.43	0.33	316
CR70	1447126	0.67	0.46	0.27	313
CR57	3273781	0.92	0.75	0.76	268
		$T=661°C$; $\epsilon=0.165$			
	0	0	0	0	344
CR69	11675	1.05	0.81	0.71	257
CR66	44680	1.09	0.90	0.82	229
CR67	233853	1.08	0.93	0.83	216
CR64	400411	1.03	0.87	0.73	237
CR60	925695	1.19	0.98	0.85	198
		$T=712°C$; $\epsilon=0.175$			
	0	0	0	0	349
CR25	11316	1.07	0.91	0.76	228
CR16	80703	1.10	0.95	0.83	212
CR14	316983	1.15	1.04	0.94	165
CR15	433517	1.06	0.94	0.83	215
CR13	1050307	1.15	1.02	0.89	178
CR7	2065827	1.16	1.01	0.90	184
CR4	2413634	1.12	1.01	0.91	183

† Data not used in fitting equation (11).
The values of ϵ_{rec} are the measured values not those calculated from equation (11).

temperature. These results are qualitatively similar to those observed in metals (e.g. Kwon and DeArdo, 1990).

As expected, for any given experiment $\sigma_{rec} > A_{rec} > \epsilon_{rec}$, The relationship between ϵ_{rec}, and σ_{rec} is non-linear (Fig. 4a), whereas that between ϵ_{rec} and A_{rec} is linear (Fig. 4b). Least squares regression of ϵ_{rec} on $(\sigma_{rec})^2$, σ_{rec} and A_{rec} yields the following fully empirical relation

$$\epsilon_{rec} = 0.2306(\sigma_{rec})^2 - 0.6086\sigma_{rec} + 1.231A_{rec} + 0.0587 \quad (11)$$

with a root mean square error ϵ_{rec} of 0.08. The fractional recovery curves generated from equation (11) by using the values of σ_{rec} and A_{rec} in each experiment to determine the modified values of ϵ_{rec} are shown in Fig. 5(a & b).

The values of σ^* obtained from the estimates of ϵ_{rec} given by equation (11) are listed in Table 1 and are plotted as a function of log anneal duration in Fig. 5(c & d). When plotted in this way the recovery curves again change in slope from shallow to steep to shallow with increasing anneal duration. At given annealing temperature, the slopes of these respective portions of the recovery curves appear to be independent of the pre-strain (Fig. 5c).

Moreover, at constant annealing temperature it appears that the position of the steep portion of the recovery curve is fixed in (σ^*, t) space, so that all the recovery curves from different pre-strains (i.e. different initial values of σ^*) merge into a single curve (Fig. 5c). The temperature dependence of the recovery behaviour is difficult to ascertain in detail because only at temperatures near 600°C can recovery be quantified over more than a very small recovery range in the experimentally accessible time scale, i.e. above 600°C recovery is nearly complete before it can be measured, whereas below 600°C it is hardly measurable at all until several weeks have passed. However, it is clear that the slope of the initial shallow portion of the recovery curves increases with increasing temperature (Fig. 5d).

Microstructural evolution

Qualitatively, the microstructural evolution during annealing is the same at all the conditions investigated, and it is only the rate at which that evolution occurs which varies with the deformation and annealing variables. The principal changes are here described with reference to Fig. 6.

After the initial deformation almost every grain in the marble is heavily twinned (Fig. 6a) even at the lowest pre-strain employed. By a pre-strain of 0.17 a crystallographic preferred orientation is strongly developed but there is only a moderate shape fabric.

During the initial part of the annealing period few changes are apparent in the optical microstructures until, after an incubation period, recrystallization begins (Fig. 6b). The duration of this incubation period decreases

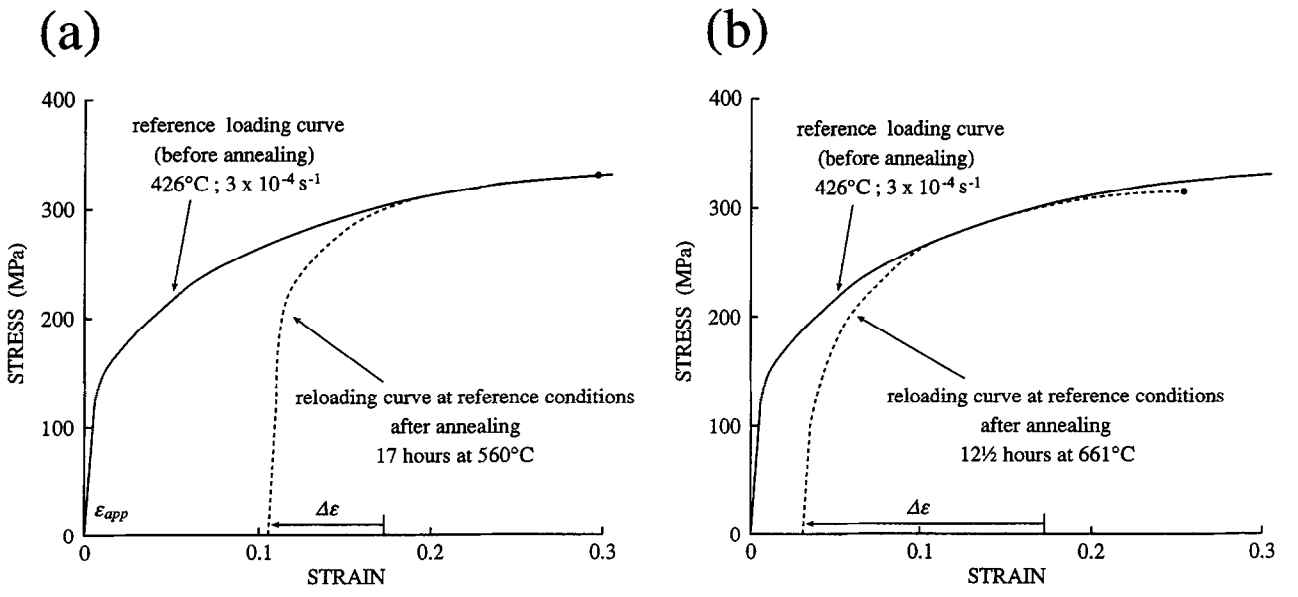

Fig. 2. Typical stress/strain curves obtained from the interrupted constant displacement-rate tests in this study. (Strains are logarithmic strains.) The reloading curves (dashed) are shown translated by the amount $\Delta\epsilon$ from the final strain obtained in the initial loading (here 0.17) to illustrate the quality of the superposition, after an initial transient, of the reloading curve onto the reference (initial) loading curve. (a) After low or moderate amounts of recovery the reloading curve superposes exactly (within experimental error). (b) After larger amounts of recovery the reloading curve departs from the reference curve at large reload strains because the total strain experienced by the sample (initial loading plus reloading) is sufficiently large for geometrically forced strain heterogeneities to compromise significantly assumptions, primarily involving the evolution of sample shape during deformation, used in the mechanical data analysis.

with increasing temperature from about 12 days at 560°C to about 2 min at 712°C (both at a pre-strain of 0.17), and decreases with increasing pre-strain from about 4 days after a pre-strain of 0.08 to about 4 h after a pre-strain of 0.27 (both at an annealing temperature of 611°C). The recrystallization nuclei may develop along twins, although almost always along spaced secondary twins and only very rarely along the dominant twin-set (Fig. 6c). New grains nucleated at the intersection of two twin sets are occasionally observed (Fig. 6d). Oriented growth of the new grains along their host twins is strongly favoured (Fig. 6e), but where several nuclei are developed along the same twin, these are not necessarily all of the same orientation (Fig. 6f). Once the whole host twin has been consumed, oriented growth of the new grains parallel to the primary twin set in the host grain is favoured (Fig. 6f). Despite an exhaustive search, no evidence of twin boundary migration occurring during the annealing was observed, although it was observed to have occurred during the pre-straining. The implication is that twin boundary migration is a dynamic recovery process *sensu stricto* (i.e. it requires the presence of a differential stress) under the experimental conditions. Of far greater significance than the spaced secondary twins as a source of recrystallization nuclei are the grain boundaries. Nuclei may develop from subgrains formed during the annealing, or from a grain boundary bulging mechanism (Fig. 6g). Once formed, some nuclei grow relatively slowly and remain approximately equant (Fig. 6h), whereas others undergo very rapid oriented growth (Fig. 6i) and become highly irregular in shape (Fig. 6j).

Recrystallization goes to completion (i.e. the old grains are completely replaced by new ones) within a log-time interval of about 1.0 irrespective of pre-strain or annealing temperature. The resulting aggregate comprises two populations of grains; one consisting of relatively small, equant grains which have approximately straight grain boundaries, the other consisting of large (although not larger than the initial grain-size), irregularly-shaped grains (Fig. 6k). The grain-sizes of both populations decrease with increasing mechanical state attained during the pre-straining but are independent of annealing temperature. The larger, irregularly-shaped grains have a shape fabric (reflecting the oriented nature of their growth), and retain the strong crystallographic preferred orientation of their parents (Fig. 6k). The smaller, equant grains do not appear to have a strong crystallographic preferred orientation, although this has not been verified by orientation measurements. Even after recrystallization is complete, the larger, irregularly-shaped grains apparently contain a significant dislocation density because subsequent annealing leads to an intensification of the subgrain substructure, a process which eventually causes, through the various subgrain recrystallization mechanisms, the break-up of the larger grains into a new generation of equant grains of a size similar to those equant grains developed in the initial phase of recrystallization. As this process proceeds the aggregate tends towards a 'foam' texture (Fig. 6l). No grain growth subsequent to recrystallization was observed in even the longest duration anneal (50 days) at the highest temperature (712°C).

(a)

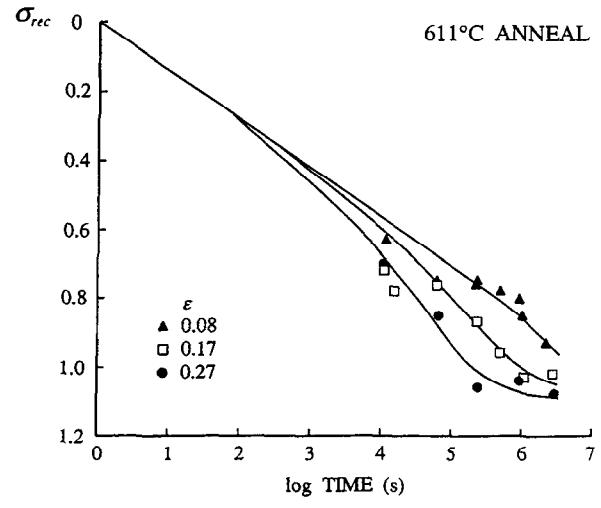
σ_{rec}
611°C ANNEAL
ε
0.08
0.17
0.27
log TIME (s)

(b)

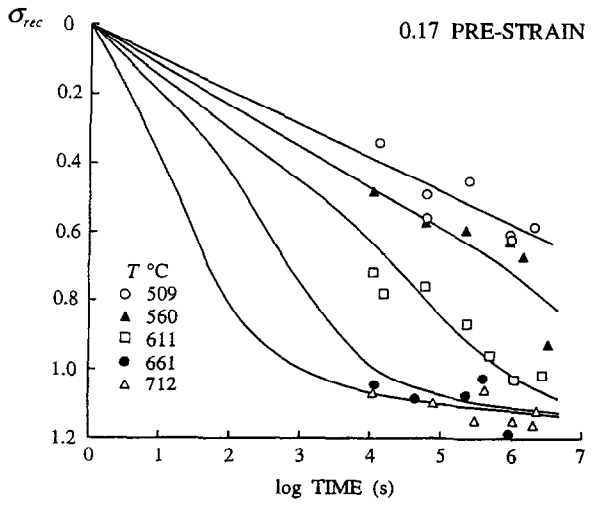
σ_{rec}
0.17 PRE-STRAIN
T °C
509
560
611
661
712
log TIME (s)

(c)

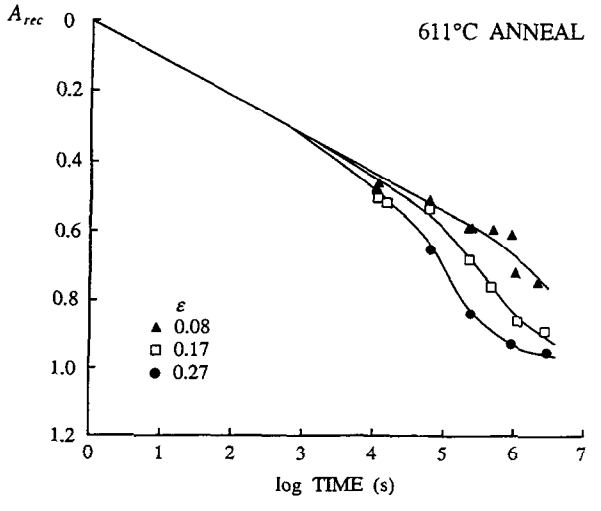
A_{rec}
611°C ANNEAL
ε
0.08
0.17
0.27
log TIME (s)

(d)

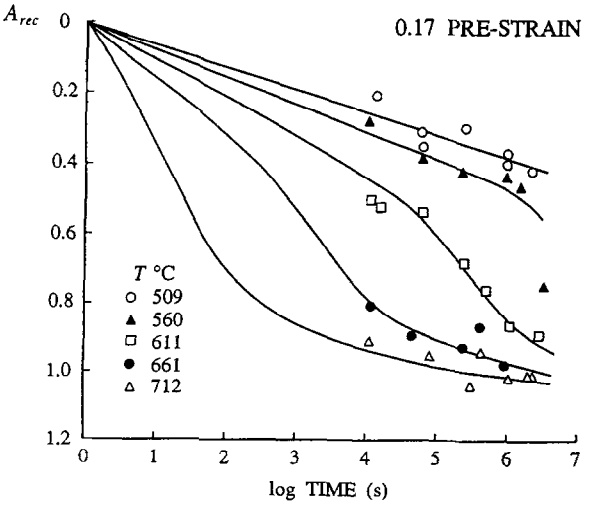
A_{rec}
0.17 PRE-STRAIN
T °C
509
560
611
661
712
log TIME (s)

(e)

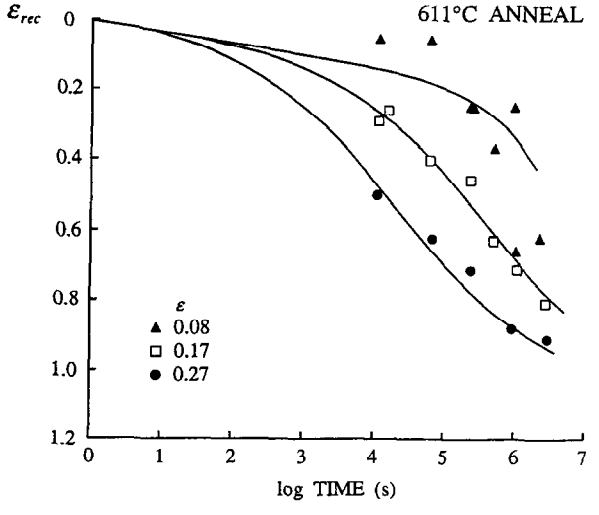
ε_{rec}
611°C ANNEAL
ε
0.08
0.17
0.27
log TIME (s)

(f)

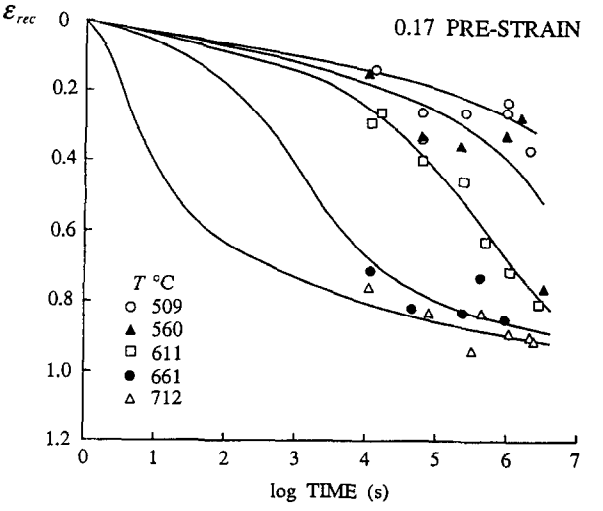
ε_{rec}
0.17 PRE-STRAIN
T °C
509
560
611
661
712
log TIME (s)

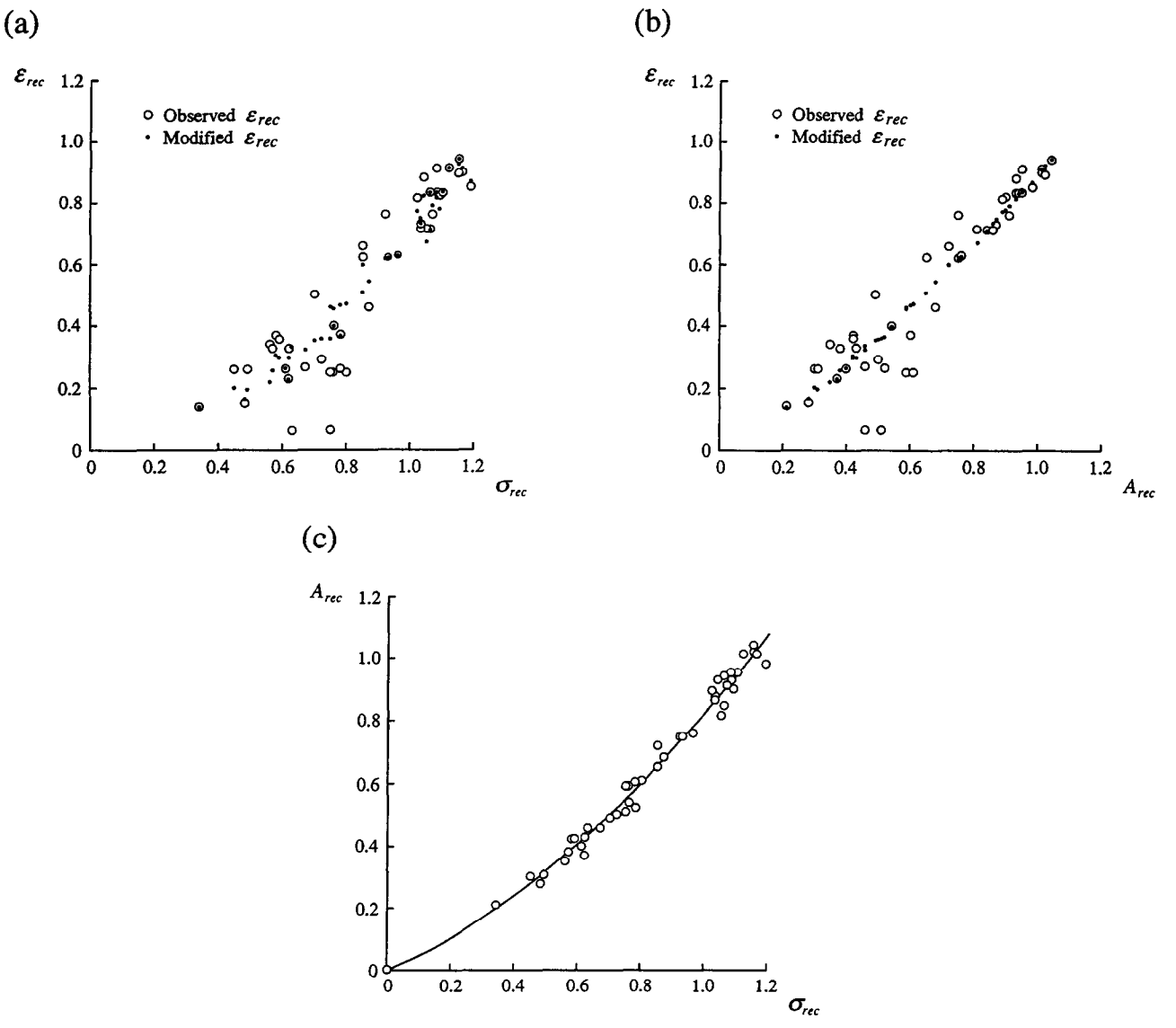

Fig. 4. Comparison of the recovery estimates based on (a) strain and stress, (b) strain and area, and (c) area and stress. The open circles are the observed values of the data. The filled circles are the strain-based estimates given by equation (11). The solid curve in (c) is the best least squares, second-order polynomial to the data presented in that figure.

DISCUSSION

Qualitatively, the most significant feature of the microstructural evolution described above is the initial phase of recrystallization when the old grains were completely replaced by new grains through processes involving significant grain boundary migration. The interval over which this phase of recrystallization occurs is shown in Fig. 5. On the fractional recovery plots (Fig. 5a & b) the recrystallization corresponds to the steep portion of the recovery curves as found in metals (Kwon and DeArdo, 1990). On the mechanical state evolution plots (Fig. 5c & d) it defines a transition between two types of recovery behaviour. The task of finding the function $\Re$ (σ^*, T) to describe the recovery behaviour would therefore seem to be one of finding a two-part function which can account for the two types of static recovery (i.e. that before and after recrystallization), and one of providing some account of the initiation and progress of recrystallization to delimit the time domain in which each part applies. To be properly constrained, such a task requires experimental data at short times (i.e.

Fig. 3. Fractional recovery as a function of anneal duration for Carrara marble using the recovery estimates given by equations (5)–(7) based on stress (a,b), area (c,d), and strain (e,f), respectively. For each estimate the curves are for constant annealing temperature after different pre-strains (a,c,e) and for different annealing temperatures after constant pre-strain (b,d,f). The curves show only trends in the data and are not fits, and at short times are guided in part by microstructural observations.

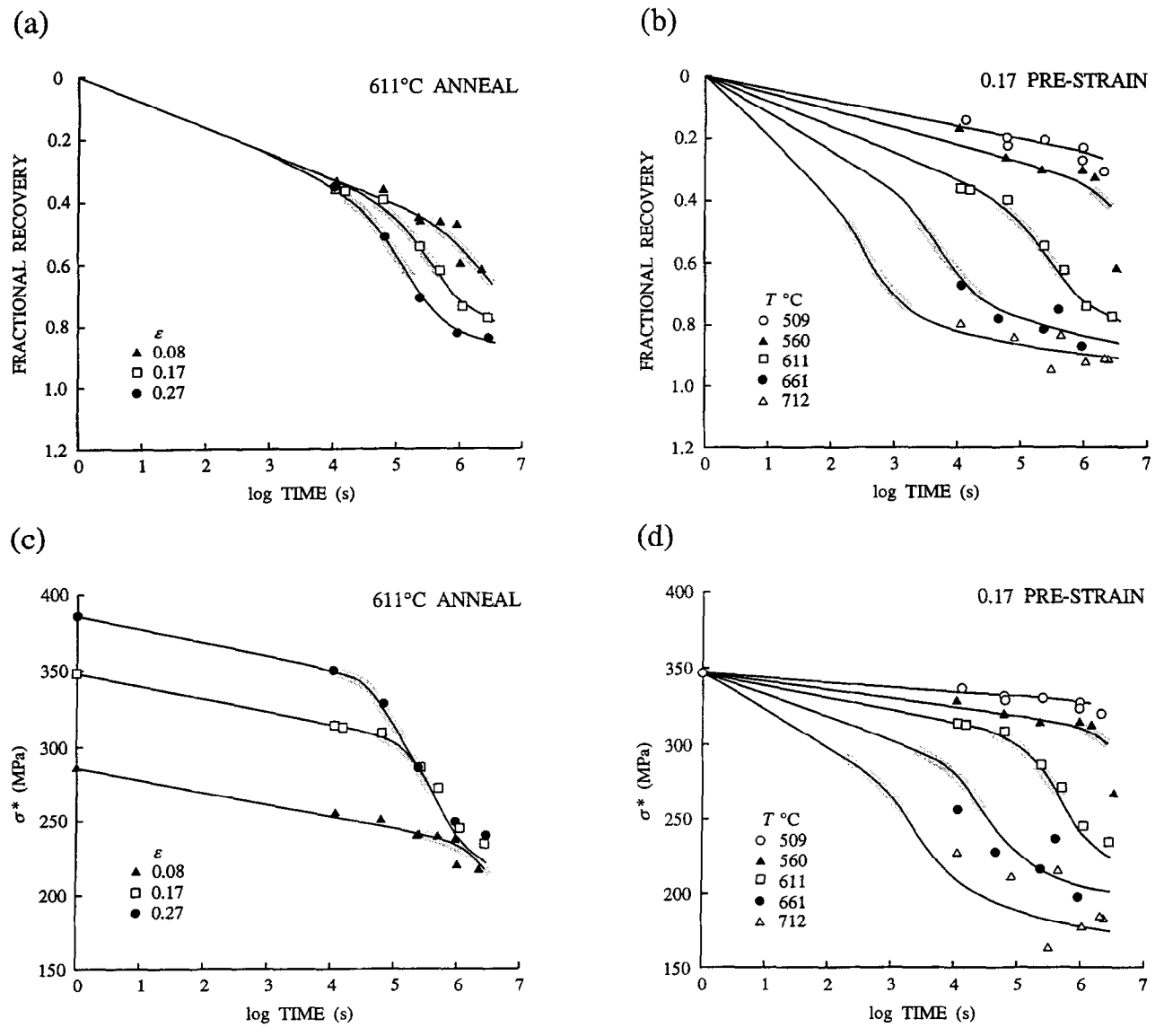

Fig. 5. The recovery curves for Carrara marble presented as: (a,b) the fractional recovery estimates given by equation (11), and (c,d) the change in mechanical state (σ^*), as a function of anneal duration. The plots are for constant annealing temperature after different pre-strains (a,c) and for different annealing temperatures after constant pre-strain (b,d). The curves show only trends in the data and are not fits (cf. Fig. 3). The shaded areas indicate the time interval over which recrystallization occurs.

$t < 10{,}000$ s) so that the recovery kinetics can be explored over a wide recovery range at more than one temperature. This in turn requires that the experiments be performed on an apparatus with an internally heated pressure vessel to minimize the period of heating from the deformation to the annealing conditions. Nevertheless, the results presented here can be used to make some pertinent observations. For convenience, in the discussion that follows, 'recrystallization' is used to refer only to the initial phase of recrystallization described in the previous paragraph. Recovery at other times (which also leads to recrystallization albeit without significant grain boundary migration), occurs through dislocation processes, and is thereby distinguished by the conventional label of 'classical static recovery'.

Static recrystallization behaviour

Conventionally, static recrystallization kinetics at given temperature are described by an Avrami-type equation

$$X = 1 - \exp[-0.69(t/t_{0.5})^n], \qquad (12)$$

where X is the volume fraction recrystallized, n is a constant depending on the nucleation and growth mechanism(s), and $t_{0.5}$ is the time required for 50% recrystallization (Laasraoui and Jonas, 1991). The application of equation (12) to the statically recrystallized microstructures obtained in this study is complicated by the fact that the progress of recrystallization tends both to be heterogeneously developed across a given sample

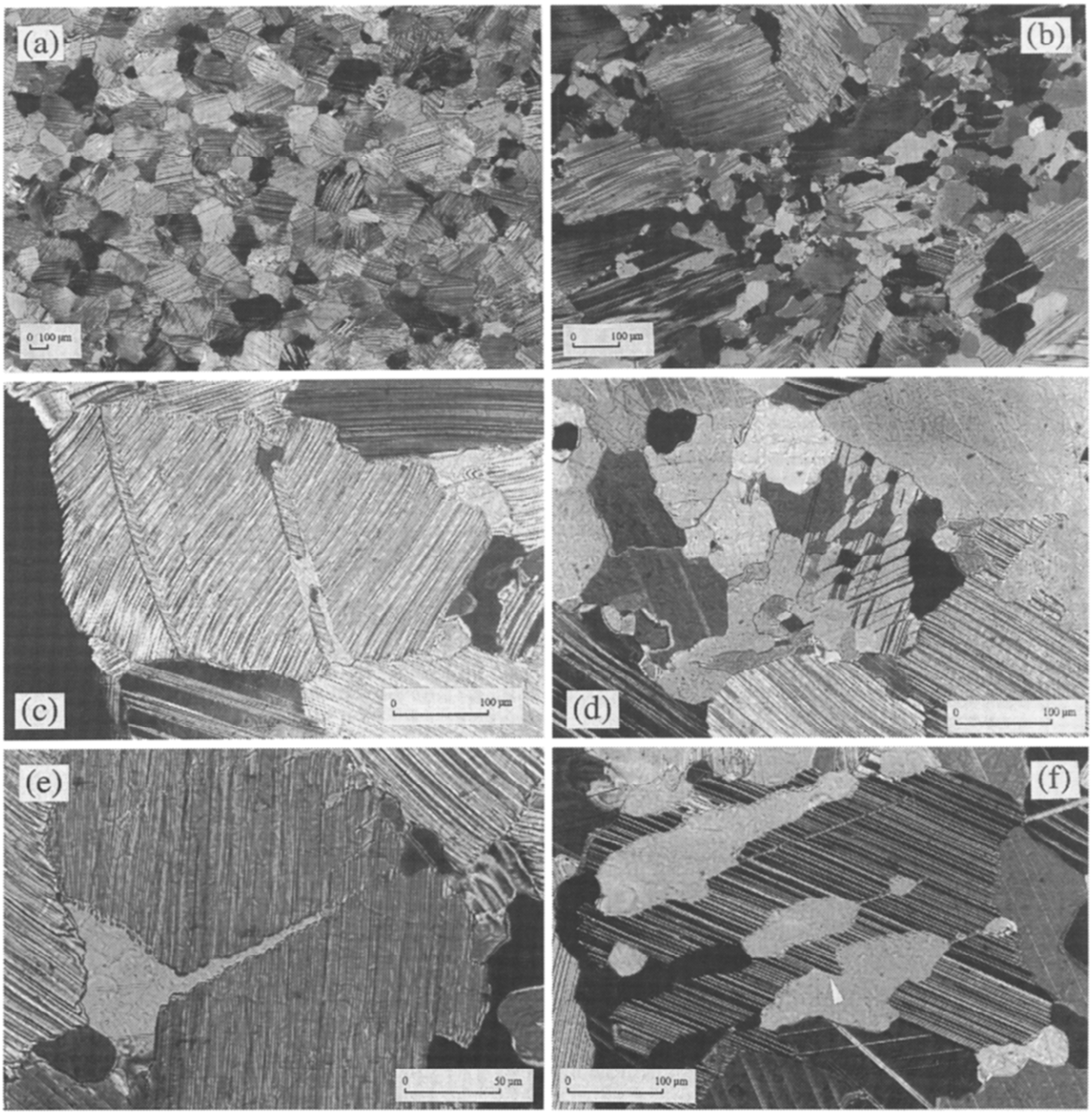

Fig. 6. The microstructural evolution during isostatic annealing. (a) The cold-worked (426°C) Carrara marble microstructure for a specimen deformed to a strain of 0.17. (b) The onset of recrystallization. The unrecrystallized grains are heavily twinned, whereas the new grains are either twin-free or contain a few cooling twins. This specimen was annealed for 28 h at 611°C after a pre-strain of 0.17. (c) The nucleation of new grains along spaced secondary deformation twins in a specimen annealed for 38 h at 611°C after a pre-strain of 0.17. (d) The nucleation of new grains at the intersections of two deformation twin sets in a specimen annealed for 50 min at 611°C after a pre-strain of 0.17. (e) Once formed the new grains which nucleate along the spaced secondary deformation twins undergo very rapid growth along the twin. This specimen was annealed for 28 h at 611°C after a pre-strain of 0.17. (f) Once the host twin has been consumed, the new grains grow into the host grain. Growth is favoured parallel to the primary twin set in that host grain (as indicated by the arrow). The different extinction positions of the new grains in this image demonstrates that the new grains formed along a given twin do not necessarily all have the same crystallographic preferred orientation. This specimen was annealed for 14 days at 611°C after a pre-strain of 0.08.

(making it difficult to determine an unambiguous value of X without measuring the whole sample), and to be poorly reproducible in detail (i.e. in terms of the value of X) between samples within the very short log-time window during which it occurs. This reflects the extreme sensitivity of the progress of recrystallization to the strain heterogeneities set up within the samples during pre-straining. Although these difficulties are sufficiently great to mean that it is not possible to determine a smooth $X(t)$ curve from a detailed quantitative analysis of the recrystallizing microstructures generated at given annealing temperature after given pre-strain, it is possible by

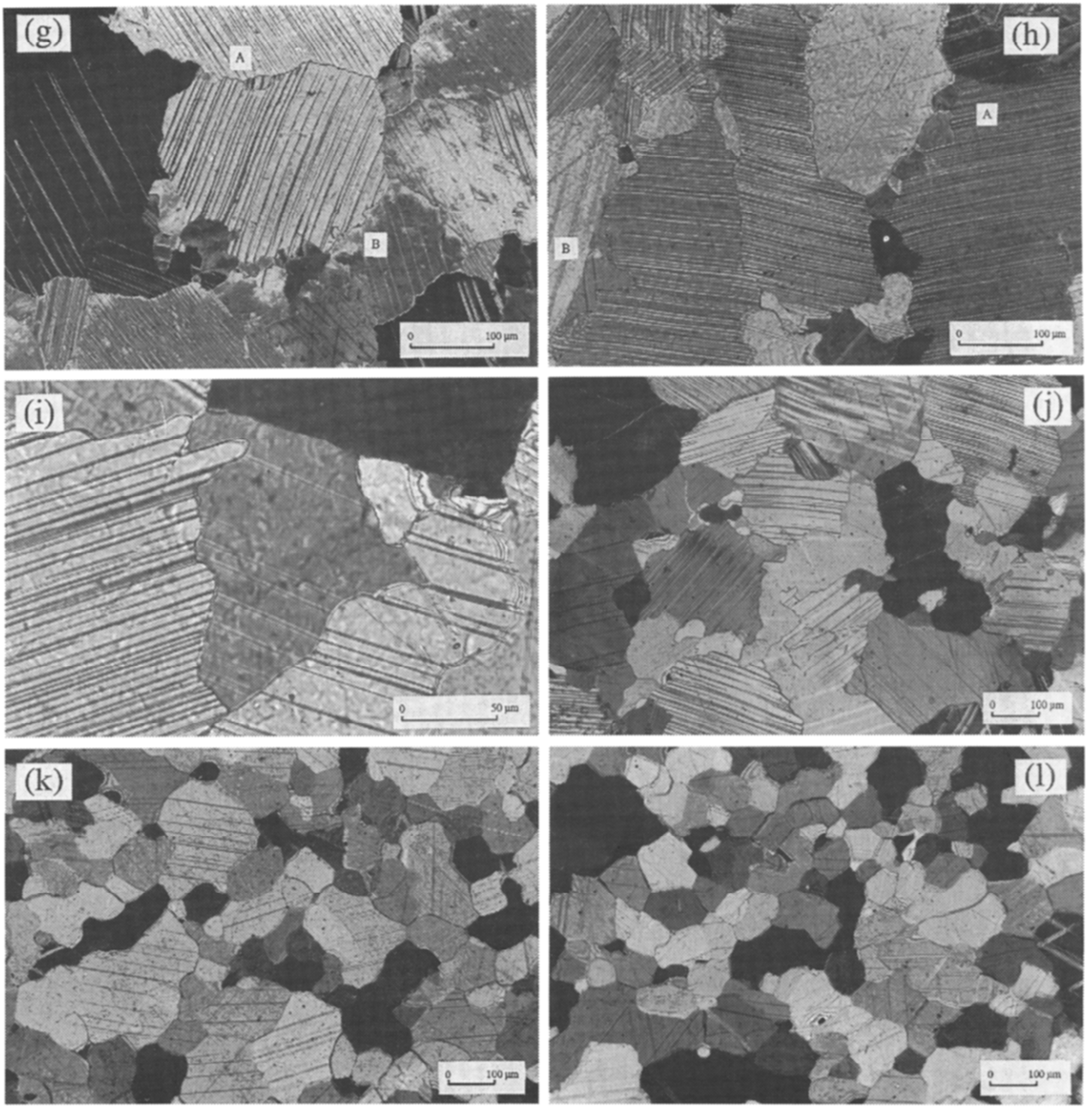

Fig. 6. (g) The nucleation of new grains along grain boundaries from progressively misorienting subgrains, A, and from grain boundary bulging, B. This specimen was annealed for 2 days at 611°C after a pre-strain of 0.17. (h) The new grains nucleated at grain boundaries either remain approximately equant, A, or undergo rapid oriented growth into the deformed grains, B. This specimen was annealed for 2 days at 611°C after a pre-strain of 0.17. (i) The growth of new grains is influenced strongly by the deformation twins in the surrounding grains. This specimen was annealed for 14 days at 611°C after a pre-strain of 0.08. (j) The rapidly growing new grains, as exemplified by the grain in the centre of this photomicrograph, become highly irregular in shape. This specimen was annealed for 14 days at 611°C after a pre-strain of 0.08. (k) The microstructure upon the completion of recrystallization. The recrystallized grains form two populations; one comprising large, irregularly-shaped grains with a grain size similar to that of the undeformed material, the other comprising smaller, relatively straight-sided, equant grains. The alignment of the cooling twins within the larger grains highlights the strong crystallographic preferred orientation of the grains in that population. This specimen was annealed for 4 days at 712°C after a pre-strain of 0.17. (l) The microstructure tends towards a foam texture upon further annealing as the larger, irregularly-shaped grains break up, through an intensification of the subgrain structure, into grains that are smaller and more equant. This specimen was annealed for 50 days at 712°C after a pre-strain of 0.17.

optical inspection to determine the onset and completion of recrystallization, and to make an estimate of the time required for 50% recrystallization. Moreover, because recrystallization occurs over a very short, but strongly temperature and mechanical state dependent, log-time window, these time estimates, made simply by optical inspection, are extremely reproducible when plotted over the full range of temperatures and mechanical states

investigated (Fig. 7). Multiple regression of the estimated times for 50% recrystallization yields

$$t_{0.5} = 4.358 \times 10^{-14}\exp(-0.0308\sigma^*)\exp(392400/RT), \quad (13)$$

where t is in s, σ^* is in MPa, T is in K and R, the gas constant, is in SI units. The root mean square error on $\ln t_{0.5}$ is 0.0577. Equation (13) is significantly simpler than previously published expressions for $t_{0.5}$ (Laasraoui and Jonas, 1991; Martin *et al.*, 1993) because, whereas in the latter the loading strain-rate, loading history and pre-strain are required to be made explicit, here they are all contained within the mechanical state variable σ^*. The apparent activation energy of 392.4 kJ mol^{-1} is similar to that observed for the self-diffusion of oxygen, carbon, and calcium in dry calcite at $T > 550$°C (Farver and Yund, 1996).

Recent efforts to combine Hart's description of inelastic deformation with the theory of the thermodynamics of irreversible processes to determine the conditions for the onset of recrystallization (Poliak and Jonas, 1996) point the way forward for incorporating recrystallization into the formulation of an appropriate recovery function. The results described above provide some quantitative insight into the progress of recrystallization once initiated, but a more detailed investigation of the recrystallization kinetics to evaluate the terms in expressions like equation (12) must be carried by other means. Clearly such an investigation must incorporate some account of the relative significance of the two types of recrystallization observed here (i.e. that producing the larger, irregularly-shaped grains and that producing the smaller, equant grains) and its dependence upon σ^* and T.

Classical static recovery behaviour

There have been few attempts to provide a general description of classical static recovery kinetics, i.e. recovery ascribed to dislocation annihilation and reorganization. A common observation is that during the initial stages of such recovery there is a logarithmic decay in material properties such that

$$x = a - b\ln t, \quad (14)$$

where x is the material property (e.g. the yield stress), and a and b are constants at given annealing temperature, but where b has an Arrhenius dependence on temperature (Honeycombe, 1968). Equation (14) describes the decay in σ^* prior to recrystallization shown in Fig. 5(c & d), with b being independent of pre-strain, and increasing with increasing temperature. However, after recrystallization the decay of σ^* with log-time is non-linear as it must be if σ^* is not to decrease ultimately to zero and then become negative.

The difference between the decay of σ^* before and after recrystallization suggests that treatment of the recovery behaviour within the framework of a single mechanism such as implied by equation (14) is inadequate. The microstructural observations suggest that prior to recrystallization the recovery behaviour is controlled by the annihilation and rearrangement of dislocations to form a subgrain structure, i.e. it is controlled by the decreasing dislocation density within that emerging cell/subgrain structure. The onset of recrystallization effectively serves to increase the rate of this process so that when the recrystallization is complete the subgrain structure is well-developed. Once the recrystallization is completed, recovery is controlled by subgrain growth. Nes (1995) has

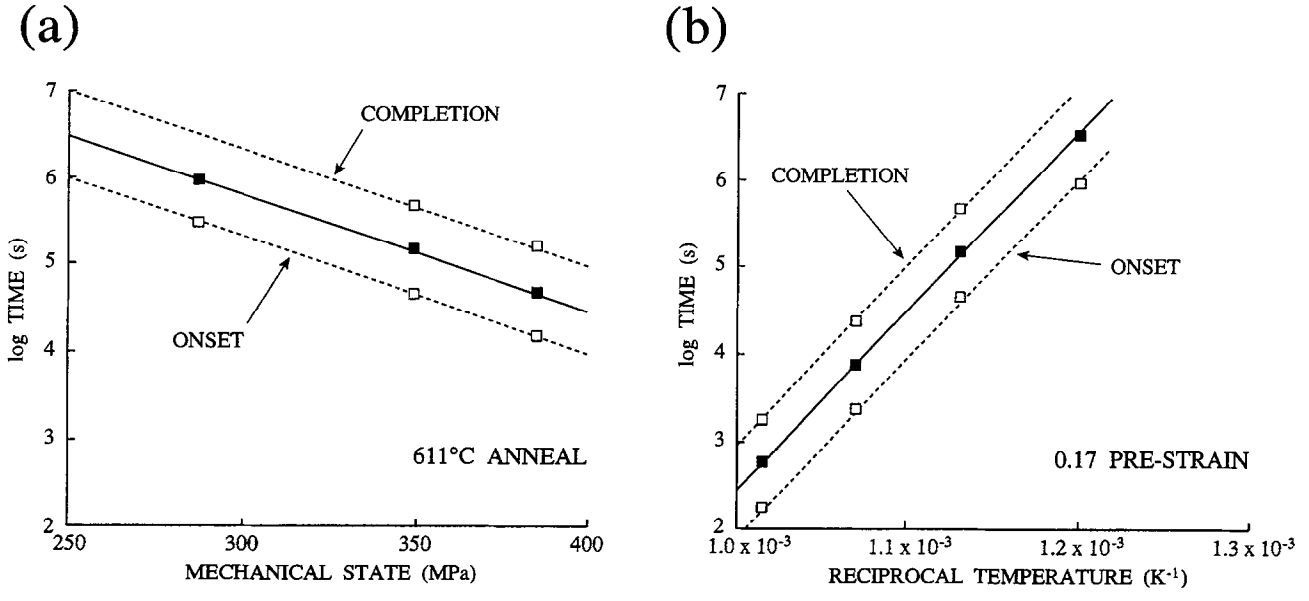

Fig. 7. The progress of static recrystallization in cold-worked Carrara marble, plotted (a) at given annealing temperature as a function of final mechanical state attained during the cold-working, and (b) at given pre-strain (i.e. mechanical state) as a function of reciprocal annealing temperature. The solid curves are fits (equation 13) to the estimated times for 50% recrystallization. The dashed curves bound the interval between the onset and completion of recrystallization.

developed several expressions describing classical static recovery behaviour, in the first instance by treating it either as some weighted combination of the contributions of these two elements (i.e. substructure formation and substructure growth) or as a transition from a situation of dominance by one to dominance by the other, and in the second instance by incorporating various possible mechanisms for the evolution of dislocation density within a subgrain network and for subgrain growth. Such expressions may be of considerable utility in devising a general form for $\Re(\sigma^*, T)$. However, before this can be attempted reliably there is a need to consider more closely the correlation between the magnitude of σ^* and both dislocation density and subgrain size. It may be that at high temperatures where subgrain structures can readily develop, there is a need for more than one mechanical state variable, perhaps one correlating with mobile dislocation density and the other with subgrain size.

CONCLUSIONS

The evolution of the mechanical properties and microstructures of cold-worked (426°C) samples of Carrara marble during isostatic annealing at 500–700°C have been investigated, and the results interpreted from the perspective of Hart's state variable description of inelastic deformation. The general features of the annealing behaviour of Carrara marble are found to be similar to those observed in metals.

(1) The rate of recovery is initially slow and is apparently controlled by the annihilation of dislocations or by their reorganization into a subgrain structure. During this stage of recovery there is a logarithmic decay in the mechanical state of the Carrara marble.

(2) The development of the subgrain structure is accelerated by recrystallization. The onset of recrystallization is uniquely specified by the mechanical state at the start of annealing and by the annealing temperature. The nuclei for the recrystallized grains form primarily in the grain boundaries but may also form along spaced secondary deformation twins. Once formed the nuclei either grow slowly and produce equant grains, or they undergo very rapid oriented growth and develop an irregular shape. Recrystallization goes to completion within a log-time interval of 1.0 and results in a microstructure which substantially retains the crystallographic preferred orientation of its precursor.

(3) Upon completion of recrystallization the larger, irregularly-shaped grains slowly break up into smaller equant grains by an intensification of the subgrain structure. During this stage of recovery the mechanical state σ^* of the Carrara marble decays such that $d\sigma^*/d(\log t)$ continuously decreases.

(4) The use of Hart's mechanical state variable simplifies the description of annealing behaviour by accommodating within one variable all the factors in the thermomechanical history of the material which affect that behaviour. Moreover, the results are sufficiently systematic to suggest that a general function describing static recovery and recrystallization can be readily formulated within the terms required by Hart's state variable description of inelastic deformation. However, for this task to be properly constrained there is a need both for data from shorter anneal duration experiments than it was possible to obtain in this study, and for a closer investigation of how the magnitude of the mechanical state variable correlates with microstructural features such as dislocation density and subgrain size.

Acknowledgements—The experimental work reported here was conducted in the Rock Deformation Laboratory, Department of Earth Sciences, University of Manchester, during tenure of a NERC Postdoctoral Research Fellowship (GT5/92/GS/2). It has been written up during tenure of a Royal Society University Research Fellowship. The work has benefited from discussions with Ernie Rutter and, with respect to the twinning microstructures that were observed, with Bob Ward. In addition the attention of Rob Holloway to the maintenance and upgrading of the deformation apparatus used for the experiments made an essential contribution to the quality of the data obtained. The constructive reviews of Steven Wojtal, Ben van der Pluijm, and Hans de Bresser led to a number of improvements to the text.

REFERENCES

Alexopoulos, P. S., Cho, C. W., Hu, C. P. and Li, C.-Y. (1981) Determination of the anelastic modulus for several metals. *Acta metallurgica* **29**, 569–577.

Alexopoulos, P. S., Keusseyan, R. L., Wire, G. L. and Li, C.-Y. (1982) Experimental investigation of nonelastic deformation emphasizing transient phenomena by using a state variable approach. In *Mechanical Testing for Deformation Model Development*, eds R. W. Rohde, and J. C. Swearengen. *American Society for Testing and Materials, Special Technical Publication* **765**, 148–184.

Covey-Crump, S. J. (1992) Application of a state variable description of inelastic deformation to geological materials. Unpublished Ph.D. thesis. London University.

Covey-Crump, S. J. (1994) The application of Hart's state variable description of inelastic deformation to Carrara marble at $T<450$°C. *Journal of geophysical Research* **99**, 19793–19808.

Farver, J. R. and Yund, R. A. (1996) Volume and grain boundary diffusion of calcium in natural and hot-pressed calcite aggregates. *Contributions to Mineralogy & Petrology* **123**, 77–91.

Hart, E. W. (1970) A phenomenological theory for plastic deformation of polycrystalline metals. *Acta metallurgica* **18**, 599–610.

Hart, E. W. (1976) Constitutive equations for the nonelastic deformation of metals. *Journal of Engineering Materials and Technology* **98**, 193–202.

Hart, E. W. (1984) A micromechanical basis for constitutive equations with internal state variables. *Journal of Engineering Materials and Technology* **106**, 322–325.

Honeycombe, R. W. K. (1968) *The Plastic Deformation of Metals*. Edward Arnold, London.

Jackson, M. S., Cho, C. W., Alexopoulos, P. and Li, C.-Y. (1981) A phenomenological model for transient deformation based on state variables. *Journal of Engineering Materials and Technology* **103**, 314–325.

Korhonen, M. A., Hannula, S.-P. and Li, C.-Y. (1987) State variable theories based on Hart's formulation. In *Unified Constitutive Equations for Creep and Plasticity*, ed. A. K. Miller, pp. 89–137. Elsevier Applied Science, London, 89–137.

Kwon, O. and DeArdo, A. J. (1990) On the recovery and recrystallization which attend static softening in hot-deformed copper and aluminum. *Acta metallurgica et materialia* **38**, 41–54.

Laasraoui, A. and Jonas, J. J. (1991) Recrystallization of austenite after deformation at high temperatures and strain-rates — analysis and modeling. *Metallurgical Transactions* **22A**, 151–160.

Martin, S., Gutierrez, I. and Urcola, J. J. (1993) Static recrystallization kinetics of commercial aluminium: influence of hot deformation mode. *Materials Science and Technology* **9**, 874–881.

Miller, A. K. (ed.) (1987) *Unified Constitutive Equations for Creep and Plasticity*. Elsevier Applied Science, London.

Nes, E. (1995) Recovery revisited. *Acta metallurgica et materialia* **43**, 2189–2207.

Poliak, E. I. and Jonas, J. J. (1996) A one-parameter approach to determining the critical conditions for the initiation of dynamic recrystallization. *Acta materialia* **44**, 127–136.

Rutter, E. H. (1995) Experimental study of the influence of stress, temperature, and strain on the dynamic recrystallization of Carrara marble. *Journal of geophysical Research* **100**, 24651–24663.

Rutter, E. H. and Brodie, K. H. (1988) Experimental 'syntectonic' dehydration of serpentinite under conditions of controlled pore water pressure. *Journal of geophysical Research* **93**, 4907–4932.

Sneddon, I. N. (1957) *Elements of Partial Differential Equations*. McGraw-Hill, New York.

Stone, D. S. (1991) Scaling laws in dislocation creep. *Acta metallurgica et materialia* **39**, 599–608.

Yamada, H. (1977) Effect of heat treatment on the mechanical state of 20% cold worked Type 316 austenitic stainless steel. *Scripta metallurgica* **11**, 321–325.